

INVESTIGATION ON THE TRANSVERSE EMITTANCE GROWTH OF INTENSE BEAM DURING BUNCHING

P. Sing Babu^{*}, A. Goswami[†] and V. S. Pandit[#]

Variable Energy Cyclotron Centre, 1- AF, Bidhannagar, Kolkata-700 064, India

Abstract

A 2D particle in cell (PIC) code is developed to study the transverse dynamics of space charge dominated beam during bunching. The linear increase in the current within the specified bunch width due to density modulation during the transport is included in the method. Simulation shows emittance growth during bunching induced by the space charge effect for nonuniform distribution.

INTRODUCTION

In high current accelerators for example cyclotron, only a fraction of the injected dc beam from an external ion source is accepted for further acceleration. The typical value of phase acceptance of cyclotron is ~ 10 % of an rf cycle. Beam current in this phase acceptance can be improved by using a suitable buncher in the injection line [1-3]. To compress the dc beam longitudinally one needs to impose a velocity modulation at the buncher gap. In the case of high intensity beams, increase of current in the specified bunch affects the transverse dynamics. In general, the collective process in intense beams is provided by the Vlasov-Maxwell equations [4]. The average behaviour of transverse beam dynamics during beam bunching is studied using envelope equations [5-8]. The transverse component of space-charge force increases after the buncher because of the compression of the beam as the beam advances in the transport line. Generally a PIC simulation is used for self-consistent study of space charge dominated beam dynamics [9-12]. However, in the case of bunching where longitudinal compression takes place and optimization of transport parameters are also involved, such calculations become cumbersome and take long time. In the present paper we have studied the transverse beam dynamics in the presence of beam bunching using a linear increase of beam current in the specified bunch width from the buncher position to the time focus. The evolution of beam envelope and emittance growth have been estimated for various initial particle distributions.

PIC SIMULATION METHOD

In the PIC method, the beam is represented by a large number of macroparticles. Each macroparticle usually represents many individual ions maintaining the charge to mass ratio of a single ion [9]. Equations of motion of macroparticles are solved in the laboratory frame. After passing through the buncher gap the current in the bunch increases which also increases the line charge density. We have used a linear increase of beam current in the specified bunch width from the buncher position to the

time focus. If the current in the bunch at location s is $I(s)$ then the space-charge density of each macroparticle becomes

$$Q_{xy}(s) = Q_{xy}(0)I(0)\left(1 + \frac{(\eta-1)s}{L}\right). \quad (1)$$

Where $Q_{xy}(0)$ is the density of each macroparticle at $s=0$, η is the bunching factor, L is the drift distance of time focus from buncher.

The equations of motion of macroparticles in the laboratory coordinate system are given by,

$$\frac{d\mathbf{r}_\perp}{ds} = \frac{\mathbf{v}_\perp}{\beta c} \quad (2a)$$

$$m(s)\frac{d\mathbf{v}_\perp}{ds} = \frac{q(s)}{\gamma^2 \beta c} \mathbf{E}^{sc} + q(s)\mathbf{v} \times \mathbf{B}^{ext} \quad (2b)$$

where $\mathbf{v} = (\mathbf{v}_\perp, v_\parallel)$ is the component of the velocity in transverse and longitudinal direction, $\mathbf{r}_\perp = (x, y)$, $\mathbf{v}_\perp = (v_x, v_y)$ are the component of the position and velocity in transverse direction respectively. $q(s) = qI(s)/I(0)$ and $m(s) = mI(s)/I(0)$ are the charge and mass of each macroparticle at location s . The terms \mathbf{E}^{sc} and \mathbf{B}^{ext} are the self-electric field and external magnetic field respectively. In the analysis, we have included the effect of self-magnetic field by multiplying a factor of $1/\gamma^2$ in the electrostatic space-charge force terms.

RESULTS

The injection system consists of a 2.45 GHz microwave ion source and a solenoid based transport system to focus and match the beam at the entrance of spiral inflector [13, 14]. The schematic diagram of the transport system is shown in Fig. 1.

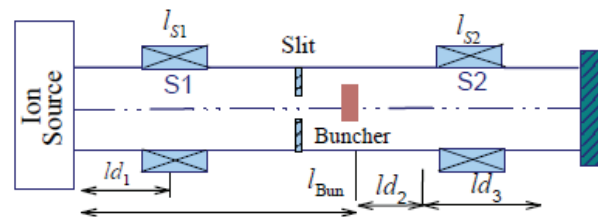


Figure 1: Schematic diagram of the beam bunching system.

^{*}psb@vecc.gov.in, [†]animesh@vecc.gov.in, [#]pandit@vecc.gov.in

Injection system is axisymmetric, consisting of two solenoid magnets S1 and S2, with physical lengths of $l_{s1}=l_{s2}=40$ cm. A slit at $s = 135$ cm is used to reject the unwanted portion of the beam. A sinusoidal buncher is located just before the second solenoid S2.

In the present 2D PIC simulation, the transverse calculation region is fixed at $12.8 \text{ cm} \times 12.8 \text{ cm}$, and it is assumed that the beam pipe is perfectly conducting. The calculation region is divided into uniform rectangular meshes with mesh points $n_x = n_y = 128$. We have used a step size $\Delta s = 1 \text{ mm}$ in the axial direction and 77,000 macroparticles after running many test simulations. The initial beam parameters used in the numerical simulations are: rms beam size = 1.25 mm, rms beam divergence = 0 mrad, beam energy = 100 keV and rms emittance $\varepsilon(0) = 13.70 \text{ mmmrad}$. For 10 mA proton beam at 100keV, to have a waist at $s = 135$ cm and $s = 272$ cm, the required peak magnetic fields in solenoids S1 and S2 should be 3.03 kG and 3.0 kG respectively. The location of the centre of S1 and S2 are at $s = 60$ cm and $s = 210$ cm from the ion source. The optimised beam line parameters with bunching satisfying the matching condition at the time focus are: $ld_2 = 35.5$ cm, $l_{s2} = 35$ cm, $B_2 = 3.418$ kG. The results of PIC simulation for 10mA beam current in these two cases for different beam distributions are shown in Figs. 2 to 5.

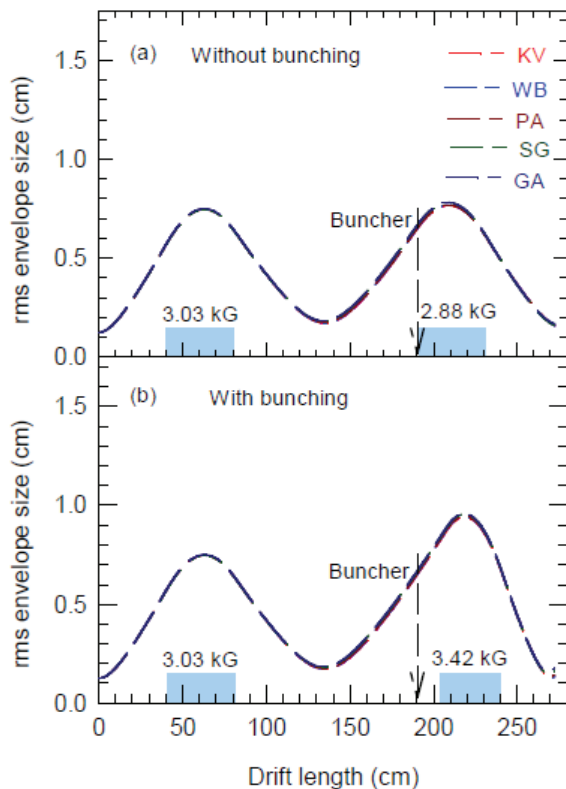


Figure 2: Evolution of the rms beam size with and without bunching using 2D PIC method with optimised position of solenoid S2.

The evolution of the rms envelope size for K-V (KV), waterbag (WB), parabolic (PA), semi-Gaussian (SG) and Gaussian (GA) distributions with and without bunching is shown in Fig. 2a. The simulation results shown in Fig. 2a indicate that evolution of rms beam envelope of dc beam is independent of the type of the beam distribution as expected from theory of space charge dominated beams. This fact is also true in the case of beam bunching which is shown in Fig. 2b. The formation of beam waist at the same location and necessity of different transport parameters for two cases clearly indicates the effect of increased space charge force during the bunching on the transverse beam dynamics.

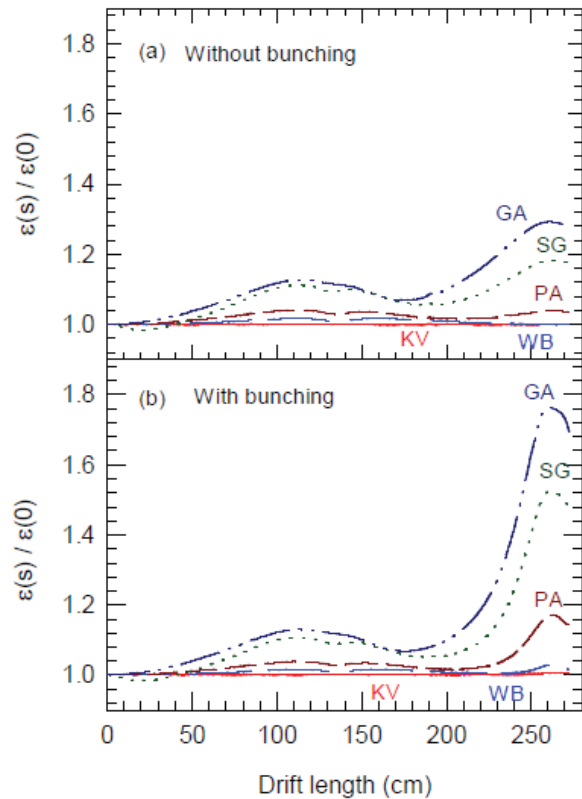


Figure 3: Comparison of rms emittance as a function of drift length with and without bunching for five different beam distribution in the transverse phase space.

Though the evolution of rms envelope is independent of beam distribution the dynamical picture changes significantly with nonuniform distribution. The evolution of rms emittance with and without beam bunching for different distributions is shown in Fig. 3. It is evident from the figure that the emittance grows significantly when nonlinearity in the space charge force is enhanced by the non-uniformity of the beam distribution and shows an oscillating pattern in both cases. For K-V distribution the transverse emittance is unaffected by the longitudinal compression. In the case of other distributions emittance growth arises due to nonlinear space charge force and results into redistribution of the beam particles. The effect is more in the case of Gaussian distribution. The reduction in the emittance during the initial part of the transport for

the semi-Gaussian distribution is due to the relaxation. In the case of bunching with Gaussian distribution the emittance reaches to a very high value almost ~ 1.8 times the initial value near the time focus where the current in the bunch is maximum and then it decreases as the current in the specified bunch width reduces. Different patterns of emittance evolution near the time focus for the two cases clearly indicate the effect of longitudinal compression on the transverse dynamics. Since the transverse matching point in the subsequent accelerator section is near the time focus, the contribution of growth in the emittance due to longitudinal compression should be within the acceptable limit to avoid the beam losses.

The distribution of beam in the transverse real space and phase space at the time focus ($s = 272$ cm) with and without bunching for K-V and Gaussian distributions are shown in Fig. 4 and Fig. 5. Simulation results show no deformation in the real and phase space distributions at the time focus for K-V distributions even in the presence of bunching. However, in the case of other distributions nonlinear space charge forces of intense beam produce strong emittance growth and halo formation due to mismatch of the beam distribution with linear focussing field and this deformation is more in the case of bunching. The phase space of the beam is more twisted where the non-uniformity in the beam distribution is increased and we see a redistribution of the beam particles with large growth and distortion in the phase space.

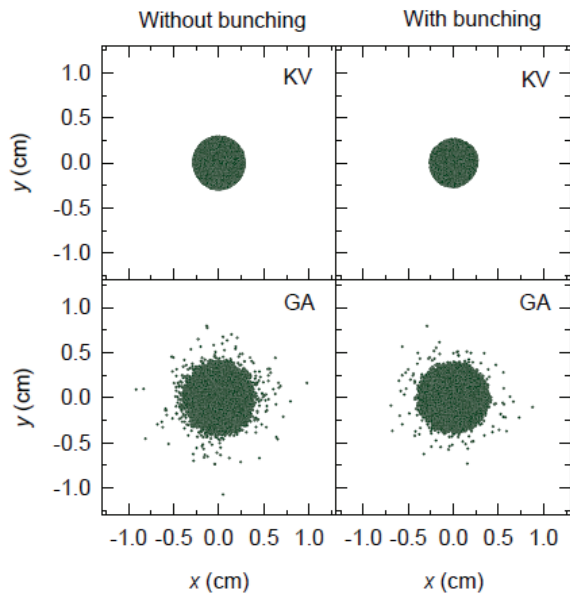


Figure 4: Real space distribution of macroparticles at $s = 272$ cm without bunching and with bunching.

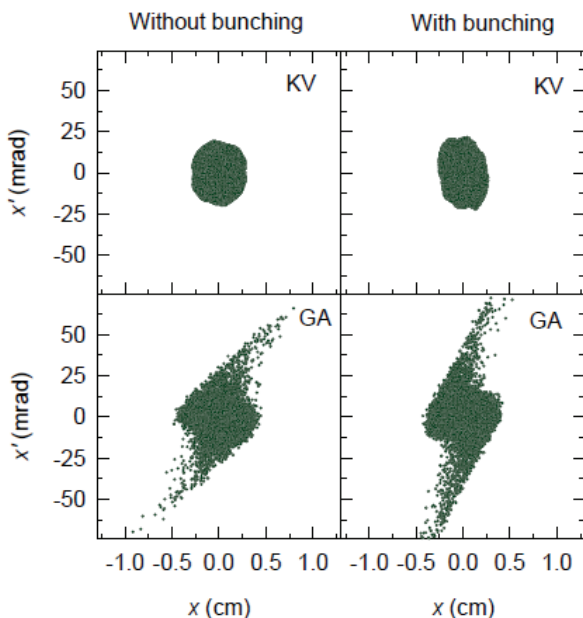


Figure 5: Phase space distribution of macroparticles at $s = 272$ cm without bunching and with bunching.

CONCLUSION

We have studied the transverse beam dynamics during the beam bunching using a 2D PIC simulation method. The linear increase in the current within the specified bunch width during the transport is included in the PIC method. It is observed that the evolution of rms envelope size is independent of the type of the distribution. Large emittance growth and halo formation are observed with nonuniform distribution during the bunching induced by the mismatch of beam distribution with the focusing field. The evolution patterns of emittance near the time focus clearly indicate the effect of longitudinal compression on the transverse dynamics.

REFERENCES

- [1] V. S. Pandit, P. R. Sarma, R. K. Bhandari, Nucl. Instrum. Methods Phys. Res. A 276 (1989) 21.
- [2] C. Goldstein, A. Laisne, Nucl. Instrum. Methods 61 (1968) 221.
- [3] V. S. Pandit, P. R. Sarma, Nucl. Instrum. Methods Phys. Res. A 462 (2001) 349.
- [4] R. C. Davidson and H. Qin, Physics of Intense Charged Particle Beams in High Energy Accelerators (World Scientific, Singapore, 2001).
- [5] Hong Qin, R. C. Davidson, Phys. Rev. ST Accel. Beams 7, (2004) 104201.
- [6] J. G. Wang, D. X. Wang, and M. Reiser, Nucl. Instrum. Methods Phys. Res. A 316, (1992) 112.
- [7] P. Sing Babu, A. Goswami, V. S. Pandit, Nucl. Instrum. Methods Phys. Res. A 603, (2009) 222.
- [8] P. Sing Babu, A. Goswami, V. S. Pandit, Nucl. Instrum. Methods Phys. Res. A 642, (2011) 1.
- [9] R.W. Hockney and J.W. Eastwood, Computer Simulation Using Particles (Taylor & Francis, New York, 1988).
- [10] Y. K. Batygin, Nucl. Instrum. Methods Phys. Res. A 539, (2005) 455.
- [11] P. Sing Babu, A. Goswami, V. S. Pandit, Phys. Plasmas 19, (2012) 113112.
- [12] T. Kikuchi, K. Horioka, M. Nakajima, S. Kawata, Nucl. Instrum. Methods Phys. Res. A 577, (2007) 103.
- [13] V. S. Pandit et al., J. Phys.: Conf. Ser. 390 (2012) 012066.
- [14] P. Sing Babu, A. Goswami, V. S. Pandit, Phys. Lett. A 376, (2012) 3192.